Title

ELECTRONIC STRUCTURE OF Hg1-xCdxTe ALLOYS AMD CHARGE DENSITY CALCULATIONS USING REPRESENTIVE k-POINTS

Authors

Chadi, D.J.
Cohen, Marvin L.

Publication Date

1972-07-01

Submitted to Physical Review

LBL-1105
Preprint

ELECTRONIC STRUCTURE OF $Hg_{1-x}Cd_xTe$ ALLOYS AND CHARGE DENSITY CALCULATIONS USING REPRESENTATIVE k-POINTS

D. J. Chadi and Marvin L. Cohen

July 1972

AEC Contract No. W-7405-eng-48

LBL-1105

DISCLAIMER

LBL-1105

Electronic Structure of $Hg_{1-x}Cd_xTe$ Alloys and Charge Density Calculations Using Representative k-Points†

D. J. Chadi and Marvin L. Cohen

Department of Physics, University of California, Berkeley, California 94720

and

Inorganic Materials Research Division, Lawrence Berkeley Laboratory

Berkeley, California 94720

Abstract

We have calculated the electronic band structures and charge densities near Γ for the $Hg_{1-x}Cd_xTe$ alloy system using the empirical pseudopotential method. We find that the energy gap varies linearly with x, with the semimetal-semiconductor transition occurring at $x = 0.165$. We have calculated the total electronic charge densities of HgTe and CdTe by using a weighted sum of the charge densities at a few symmetry points in the Brillouin zone and for the non-symmetry point used by Baldereschi. We show that for a large class of semiconducting compounds the total electronic charge density can be obtained to a very high degree of accuracy using these representative k-points.

I. Introduction

The two zincblende compounds HgTe and CdTe form a continuous series of alloys[1,2,3] denoted by $Hg_{1-x}Cd_xTe$ where x is the mole fraction of CdTe in the alloy. This alloy system has been of great interest in recent years

because of the wide range of its physical properties. These alloys are a mixture of a semimetal (HgTe) with a semiconductor (CdTe); the energy gap E_G in the alloys varies continuously[4,5] between the -0.30 eV[6] "negative" gap found in HgTe to the 1.60 eV[7,8] gap found in CdTe. Narrow gap semiconducting alloys in this system have proved useful as infrared detectors.[9]

Interest in the band structures of the $Hg_{1-x}Cd_xTe$ alloys has been concentrated mainly in the region of the Brillouin zone near Γ. It is in this region where the band structures change most with alloying. The band structures for HgTe and CdTe were previously obtained[10] by using the empirical pseudopotential method.[11] In this paper we present detailed results of our calculations of the band structures of the $Hg_{1-x}Cd_xTe$ alloys along symmetry directions near Γ. The calculation is described briefly in Sec. II and the band structures are discussed in Sec. III. The charge densities for the Γ_6 and Γ_8 levels as well as the total valence band charge density near Γ are discussed in Sec. IV. The way in which the position of the Γ_6 level affects the total charge density at Γ is also discussed in Sec. IV. In Sec. V we show how the charge density at a few symmetry points can be used to calculate the total electronic charge density for each band in a crystal. The accuracy of the charge density obtained using representative k-points in this way is discussed in Sec. VI. In this section we also present the results of our calculation for the total electronic charge densities of CdTe and HgTe obtained by the approximation method described in Sec. V. The results for CdTe are compared with a previous calculation[12] using a large number of points in the Brillouin zone.

II. Band Structure Calculation

Our calculation of the band structures of the $Hg_{1-x}Cd_xTe$ alloys are based on the empirical pseudopotential method[11] and the virtual crystal approximation. The pseudopotential form factors for HgTe and CdTe were previously[10] obtained by fitting the theoretical optical reflectivity spectra to the experimental data. In the present calculation we have used the same form factors for HgTe as in our previous work.[10] The form factors for CdTe have been modified slightly because we have increased the number of plane waves used in the expansion of the wavefunctions. This was done in order to have the same number of plane waves for CdTe as for HgTe. The new form factors for CdTe were constrained to give nearly the same energy differences at Γ, X, L and K as in our previous work. The symmetric and antisymmetric form factors (in Ry) for CdTe used in the present calculations are: $V_S(|\vec{G}|^2 = 3) = -0.234$, $V_S(8) = -0.042$, $V_S(11) = 0.041$, $V_A(3) = 0.151$, $V_A(4) = 0.068$, $V_A(11) = 0.005$ and $V_A(12) = 0$. Spin-orbit interactions were included in the calculation using the Weisz scheme[13] as modified by Bloom and Bergstresser.[14] The two spin-orbit parameters were constrained to have the same ratio as the splittings in the free atoms, leaving only one spin-orbit parameter. The spin-orbit parameter[10,15] was set equal to 0.0011 (Ry) for CdTe. This gives $\Delta_0 = E(\Gamma_8) - E(\Gamma_7) = 1.02$ eV and $\Delta_1 = E(L_{4,5}) - E(L_6) = 0.6$ eV. The band structures were calculated by taking 59 plane waves into account exactly while treating an extra 54 plane waves through the Löwdin perturbation scheme.[11,16] The size of the matrix was 118 x 118 (i.e. 59 plane waves for each spin).

The pseudopotential for the alloys were taken to be the average of the HgTe and CdTe pseudopotentials. The averaging included the spin-orbit component of the Hamiltonian. The pseudopotential form factors were scaled for the small changes in the lattice constant. The lattice constants adjusted to $0^{\circ}K$ are 6.45 Å for HgTe and 6.48 Å for CdTe. The lattice constant changes almost linearly with x.[17]

III. Band Structure Results

The calculated variation of the energy gap defined as $E_G = E(\Gamma_6) - E(\Gamma_8)$ was found to be linear with x at $0^{\circ}K$. The energy gap changes sign when x increases from 0.16 to 0.17. The energy gap is -0.01 eV at $x = 0.16$ and is +0.01 eV at $x = 0.17$. The exact value of x at the semimetal-semiconductor transition point is temperature dependent. For both HgTe and CdTe $|E_G|$ decreases with temperature[5,18] thereby lowering the value of x at which the transition occurs at higher temperatures. The calculated value of x at the transition point is $x = 0.165$ at $0^{\circ}K$. This value is in excellent agreement with indirect measurements of the energy gap at low temperatures using magnetoreflection experiments,[19] and with the value obtained from the temperature dependence of the Hall constant.[20] For a highly homogeneous sample with $x = 0.161 \pm 0.003$, Groves and Harman[19] report $E_G = -0.01$ at $T \simeq 25^{\circ}K$ and $E_G = 0.01$ eV at $T \simeq 90^{\circ}K$. Vérie[20] estimates $X = 0.160 \pm 0.005$ for the transition point at low temperatures.

The calculated variation of the energy gap E_G and the spin-orbit splittings Δ_0 and Δ_1 are shown in Fig. 1, where it is seen that all these energies vary linearly with x. In Fig. 2 we show the band structures for the

top two valence bands and the first conduction band for HgTe, CdTe and two alloys near the transition point. The band structures extend from Γ to $|\vec{k}| = 0.18\,(\frac{2\pi}{a})$ in the Λ and Δ directions. Near the transition point the variation of energy with wavevector is almost linear in the region near Γ for the Γ_6 level and for the Γ_8 light mass band. This is in agreement with the band structure obtained from the Kane secular equation[21] for the case when $E_G \simeq 0$.

IV. Charge Densities near Γ

The alloys $Hg_{1-x}Cd_xTe$ have an inverted band structure similar to that of grey tin for $x < 0.165$ (Fig. 2). It is interesting to see how the position of the Γ_6 level with respect to the degenerate Γ_8 levels affects the electronic charge density near Γ. Figs. 3 and 4 show the charge densities of the Γ_6 and Γ_8 levels for HgTe and CdTe. The charge density has been evaluated at about 1600 points in a $(1,\bar{1},0)$ plane which contains both the Hg - Cd and Te sites in the primitive cell. The charge density has been normalized to $\frac{2e}{\Omega}$ where Ω is the volume of the primitive cell. The charge densities of the Γ_6 and Γ_8 levels in HgTe are nearly the same as the corresponding charge densities in CdTe, i.e. the Γ_6 and Γ_8 levels have retained their identity regardless of whether they are part of the valence or conduction bands.

In Fig. 5 we show the charge densities for the sum of the valence bands near Γ for HgTe, CdTe and the alloy $Hg_{0.167}Cd_{0.833}Te$ near the transition point. The charge densities for HgTe and CdTe have different characteristics. For HgTe, the maximum of the charge distribution occurs exactly at the Te site while for CdTe the maximum is shifted toward Cd. The difference in charge densities is directly related to the position of the Γ_6 level in these compounds. In CdTe

only the lowest valence band has largely an s-like character, but in HgTe the s-like character of the Γ_6 valence band has been added to the s-like character of the lowest valence band and one of the p-like Γ_8 bands has become the first conduction band. This difference in charge densities persists in the alloys $Hg_{1-x}Cd_xTe$; the charge density being nearly identical to the HgTe or CdTe charge densities depending on the position of the Γ_6 level. Also shown in Fig. 5 is the charge density for an alloy with a very small positive energy gap. Because of the large mixing of wavefunctions at Γ for this alloy a charge density whose characteristics are intermediate between those of HgTe and CdTe has been obtained.

The charge densities of the sum of valence bands for HgTe and CdTe are shown in Fig. 6. These charge densities were calculated using an approximation scheme described in Sec. V. The total valence band charge densities of HgTe and CdTe show a greater similarity to each other than the corresponding charge densities calculated near Γ (Fig. 5). Although for HgTe the maximum in the charge density is still at Te, the difference between CdTe and HgTe is less than is implied from the charge distributions near Γ (Fig. 5), where the Γ_6 level has greatly influenced the HgTe charge distribution.

V. Calculation of Charge Densities From a Few Representative Points in the Brillouin Zone

We can ask the question whether it is possible to obtain a good approximation to the charge density by using the charge densities of a small number of points in the Brillouin zone. Baldereschi[22] has recently proposed using

only one $\vec{k}$-point to calculate the average charge density. For fcc crystals the coordinates[21] of this point are $\frac{2\pi}{a}(0.622, 0.295, 0)$. We will show a general method of obtaining the charge density of semiconducting crystals by using the charge density calculated for a few points. We also obtain the representative point chosen by Baldereschi (referred to here as the Baldereschi point) for fcc crystals when only one point in the Brillouin zone is used for the charge density calculation. The accuracy of this method in obtaining the charge density is discussed in Sec. VI.

The procedure is to express the wavefunctions and charge densities in terms of the Wannier functions. For a given band we can express the Bloch functions in a given band in terms of the Wannier functions for that band:

$$\psi_{\vec{k}}(\vec{r}) = \frac{1}{\sqrt{N}} \sum_m e^{i\vec{k}\cdot\vec{R}_m} a(\vec{r} - \vec{R}_m)$$

where the band index has been suppressed, $\vec{R}_m$ is a lattice vector, and $a(\vec{r} - \vec{R}_m)$ is a Wannier function centered on $\vec{R}_m$. The charge density associated with this wave function is

$$\rho_{\vec{k}}(\vec{r}) = \psi^*_{\vec{k}}(\vec{r})\,\psi_{\vec{k}}(\vec{r}) =$$

$$= \frac{1}{N} \sum_{mn} e^{i\vec{k}\cdot(\vec{R}_m - \vec{R}_n)} a(\vec{r} - \vec{R}_m)\, a^*(\vec{r} - \vec{R}_n) \quad . \qquad (1)$$

The total charge density for the given band is

$$\rho(\vec{r}) = \sum_{\vec{k}} \rho_{\vec{k}}(\vec{r}) = \sum_m |a(\vec{r} - \vec{R}_m)|^2 \quad . \qquad (2)$$

The expression for $\rho_{\vec{k}}(r)$ in (1) can be written in the following way:

$$\rho_{\vec{k}}(\vec{r}) = \frac{1}{N} \sum_m |a(\vec{r} - \vec{R}_m)|^2 + \frac{1}{N} \sum_j{}' \sum_m e^{i\vec{k}\cdot\vec{R}_j} a(\vec{r} - \vec{R}_m)\, a^*(\vec{r} + \vec{R}_j - \vec{R}_m) , \tag{3}$$

where the prime in the sum over j means that the term with $\vec{R}_j = 0$ is not included in the sum. The first sum in (3) is proportional to the total charge density/and is actually the average charge density of an electron in that band. Our purpose is therefore to try to minimize the second sum in (3). To do this, consider the set of wavevectors obtained from a general wavevector $\vec{k} = (k_1\ k_2\ k_3)$ by performing <u>all</u> possible permutations and sign changes on the components. We can generate up to 48 different $\vec{k}$ vectors from a given one using these operations, which will be specified by T. The charge densities $\rho_{\vec{k}}(r)$ associated with each one of these wavevectors can be calculated easily once the charge density for one of them is known by using the symmetry operations of the Hamiltonian. The sum of charge densities obtained in this way from the charge density $\rho_{\vec{k}}(\vec{r})$ is given by

$$\sum_T \rho_{T\vec{k}}(\vec{r}) = \frac{1}{N} \sum_T \sum_m |a(r - R_m)|^2 +$$

$$\frac{1}{N} \sum_j{}' \sum_m \sum_T e^{i(T\vec{k})\cdot\vec{R}_j} a(\vec{r} - \vec{R}_m)\, a^*(\vec{r} + \vec{R}_j - \vec{R}_m) . \tag{4}$$

The first term in (4) is independent of any sign changes and permutations of $\vec{k}$ so the sum over T just multiplies this term by 48. Let $F(\vec{r})$ be the second sum in (4), then $F(\vec{r})$ can be expressed in the following way:

$$F(\vec{r}) = \frac{1}{N} \sum_j{}' e^{i\vec{k}\cdot\vec{R}_j} \sum_m \sum_T a(\vec{r} - \vec{R}_m)\, a^*(\vec{r} + T\vec{R}_j - \vec{R}_m) \quad . \qquad (5)$$

For any given $\vec{R}_j$, $T\vec{R}_j$ is a lattice vector of the same magnitude as $\vec{R}_j$, therefore the sum

$$S(\vec{r}) = \sum_m \sum_T a(\vec{r} - \vec{R}_m)\, a^*(\vec{r} + T\vec{R}_j - \vec{R}_m) \qquad (6)$$

in (5), for a given $\vec{R}_j$, remains constant under all permutations and sign changes of $\vec{R}_j$. The condition that $F(\vec{r})$ be zero can be fulfilled if we require the wavevector $\vec{k}$ to satisfy the following set of equations:

$$\sum_{|R_j| = c_m}{}' e^{i\vec{k}\cdot\vec{R}_j} = 0 \qquad m = 1, 2, 3, \ldots \qquad (7)$$

where $c_m = m^{th}$ nearest neighbor distance. In the case where two lattice vectors, such as $\vec{R}_1 = (2\,\frac{1}{2}\,\frac{1}{2})a$ and $\vec{R}_2 = (\frac{3}{2}\,\frac{3}{2}\,0)a$ in the fcc structure, have the same magnitude but the coordinates are not related by any permutations or sign changes, Eq. (7) must be satisfied for each set of lattice vectors separately.

For the fcc crystal structure, letting $\vec{k} = \frac{2}{a}(k_1\ k_2\ k_3)$, the equations to be satisfied are of the following form for the first three nearest neighbors:

$$\cos k_1 \cos k_2 + \cos k_1 \cos k_3 + \cos k_2 \cos k_3 = 0 \qquad (8)$$

$$\cos 2k_1 + \cos 2k_2 + \cos 2k_3 = 0 \qquad (9)$$

$$\cos 2k_1 \cos k_2 \cos k_3 + \cos k_1 \cos 2k_2 \cos k_3 + \cos k_1 \cos k_2 \cos 2k_3 = 0 \quad . \qquad (10)$$

The point $\frac{2\pi}{a}(0.622, 0.295, 0)$ proposed by Baldereschi satisfies (8) and (9). It is possible to show that for the fcc crystal structure there is no $\vec{k}$ which will satisfy (8) - (10) simultaneously. We can, however, use more points in the Brillouin zone in order to satisfy a greater number of the conditions of (7). In fact we can use the weighted sum of the charge density at a few points in the Brillouin zone to do this. If the charge density is going to be approximated by

$$\rho(r) = \sum_{T} \sum_{i=1} a_i \rho_{T\vec{k}_i}(\vec{r}) \tag{11}$$

then the conditions, similar to those in (7), to be satisfied are

$$\sum_{i=1}^{n} \sum_{|R_j|=c_m} a_i e^{i\vec{k}_i \cdot \vec{R}_j} = 0 \qquad m = 1, 2, 3, \ldots, \tag{12}$$

where n is the number of points being used and as before $c_m = m^{th}$ nearest neighbor distance. We must also require

$$\sum_{i=1}^{n} a_i = \frac{1}{48} \tag{13}$$

in order to have the proper normalization for the charge density. The conditions (12) are most easily satisfied by symmetry points. For example, the three symmetry points Γ, X and L can be used in this way to calculate the charge density. The charge density is then given by

$$\rho(\vec{r}) = \frac{1}{8}\rho_{\Gamma}(\vec{r}) + \frac{3}{8}\rho_{X}(\vec{r}) + \frac{1}{2}\rho_{L}(\vec{r})$$

where by $\rho_X(\vec{r})$ and $\rho_L(\vec{r})$ we mean the symmetrized charge densities at these points, (i.e., $\rho_X(\vec{r}) = \frac{1}{48} \sum_{T} \rho_{T(1,0,0)}(\vec{r})$, T being the set of 48 permutations and sign changes of the coordinates of a general wavevector; for X

this gives $\rho_X(\vec{r}) = \frac{1}{3}\left(\rho_{(1,0,0)}(\vec{r}) + \rho_{(0,1,0)}(\vec{r}) + \rho_{(0,0,1)}(\vec{r})\right)$. The symmetry points Γ, X, and L used in this combination satisfy the conditions (12) for the first three nearest neighbors and should therefore give a better charge density than the Baldereschi point; furthermore, the calculation of wavefunctions and charge densities is simpler for symmetry points than for general points. A much better scheme with three symmetry points that satisfy equations (12) for the first seven nearest neighbor distances is obtained by using a weighted sum of the symmetrized charge densities at $\vec{k}_1 = (0.5,0,0)$, $\vec{k}_2 = (1.0,0.5,0)$ and $\vec{k}_3 = (0.5,0.5,0)$ with the weighting factors $a_1 = \frac{1}{4}$, $a_2 = \frac{1}{4}$ and $a_3 = \frac{1}{2}$ respectively.

VI. Accuracy of the Representative k-Point Scheme for Charge Density

The scheme outlined in Sec. V for the calculation of charge densities from a few representative points in the Brillouin zone is clearly valid only for completely filled bands and therefore is not very useful for metals. It will give accurate results when the Wannier functions representing the bands are well-localized. The magnitude of the error in the charge density is given by $F(\vec{r})$ in (5). This error will decrease rapidly when the conditions (7) or (12) are satisfied beyond the nearest neighbor shells in which the Wannier functions are well localized. The Wannier function for a band is not unique; it is related to the Bloch functions in the band by

$$a(\vec{r}) = \sum_{\vec{k}} \psi_{\vec{k}}(r)\, e^{i\theta(\vec{k})} , \qquad (14)$$

where the $\vartheta(k)$ are arbitrary real numbers. The localization of the Wannier

function $a(\vec{r})$ depends on the choice of the $\theta(\vec{k})$. The localization of the Wannier functions for the one-dimensional case has been treated by Kohn[23] and the general case has been treated by Blount.[24]

We have used the approximation schemes described in Sec. V to calculate the electronic charge densities for HgTe, CdTe and some other semiconductors. A comparison of our results for the sum of the valence band charge densities of CdTe with previous calculations[12] using a large number of points in the Brillouin zone, shows excellent agreement between the two. The total charge densities for CdTe and HgTe were calculated in two different ways: first by using the Baldereschi point $\frac{2\pi}{a}(0.622, 0.295, 0)$ and then by using a weighted sum of the charge densities at $\frac{2\pi}{a}(0.5, 0, 0)$, $\frac{2\pi}{a}(1.0, 0.5, 0)$ and $\frac{2\pi}{a}(0.5, 0.5, 0)$, as described in Sec. V. For CdTe the total charge densities obtained in these two ways were found to agree with one another and with the 71 point calculation[12] to about $\pm$ 1%. The sum of the valence band charge densities for HgTe and CdTe obtained in this way are shown in Fig. 6.

The accuracy of the approximation schemes is less for the individual valence band charge densities than for the sum of the valence band charge densities. The scheme using the weighted sum of charge densities at $(0.5, 0, 0)$, $(1, 0.5, 0)$ and $(0.5, 0.5, 0)$ (in units of $\frac{2\pi}{a}$) gives individual valence band charge densities to an accuracy of $\pm$ 5% for many crystals. The accuracy of the Baldereschi point is lower than the three point scheme as may be expected. The reason why the total charge density turns out to be more accurate than individual band charge densities is that even though the

Wannier functions for the individual bands may not be localized, we can construct a set of composite Wannier functions from these bands such that they are more localized and such that they will give the total charge density. For n interacting bands we can construct n composite Wannier functions:

$$a_i(\vec{r}) = \frac{1}{\sqrt{N}} \sum_{\vec{k}} \sum_{m=1}^{n} U_{im}(\vec{k}) \psi_{k,m}(\vec{r}) \quad , \quad i = 1, \ldots, m \quad , \qquad (15)$$

with the requirement that $U(\vec{k})$ be a unitary matrix for each $\vec{k}$. These Wannier functions are constructed from a combination of Bloch functions from different bands m, and satisfy the usual properties of Wannier functions. The Bloch wavefunctions can be expressed in terms of these composite Wannier functions:

$$\psi_{\vec{k},m}(\vec{r}) = \frac{1}{\sqrt{N}} \sum_{i=1}^{n} \sum_{j} U^*_{im}(\vec{k}) e^{i\vec{k}\cdot\vec{R}_j} a_i(\vec{r} - \vec{R}_j) \quad . \qquad (16)$$

The sum of the charge densities of the n bands is then given by

$$\sum_{m=1}^{n} \sum_{k} \psi^*_{k,m}(r) \psi_{k,m}(r) = \sum_{i=1}^{n} \sum_{j} |a_i(\vec{r} - \vec{R}_j)|^2 \quad . \qquad (17)$$

This expression is similar to (2) with the exception that in (17), $a_i(\vec{r})$ does not represent the Wannier function of any given band. There is considerably more freedom in constructing the composite Wannier function (15) than the simple Wannier functions (14). This extra degree of freedom can be used to make the composite functions very localized particularly if the bands from which they are constructed do not interact strongly with other bands. The approximation schemes described in Sec. V can be easily extended to these

new Wannier functions for the calculation of the total charge density. The representative points in the Brillouin zone giving the total charge density are again found to satisfy the conditions (7) or (12). These localized Wannier functions provide at least some explanation for the fact that the calculation of the valence band charge densities using only a few representative points turn out to be so accurate.

Acknowledgements

We would like to thank Carmen Varea de Alvarez and John D. Joannopoulos for useful discussions and helpful comments. Part of this work was done under the auspices of the U. S. Atomic Energy Commission.

References

†Supported in part by National Science Foundation Grant GP 13632.

1. W. D. Lawson, S. Nielson, E. H. Putley, and A. S. Young, J. Phys. Chem. Solids 9, 325 (1959).
2. J. L. Schmit and C. J. Speerschneider, Infrared Phys. 8, 247 (1968).
3. D. Long, in Energy Bands in Semiconductors (John Wiley & Sons, Inc., New York, 1968), pp. 156-159.
4. I. Melingailis and A. J. Strauss, Appl. Phys. Lett. 8, 179 (1966).
5. M. W. Scott, J. Appl. Phys. 40, 4077 (1969).
6. C. R. Pidgeon and S. H. Groves, Proceedings of the 1967 Int. Conf. on II-VI Semiconducting Compounds, D. G. Thomas, ed., (Benjamin, N.Y., 1967), p. 1080.
7. D. G. Thomas, J. Appl. Phys. 32, 2298 (1961).
8. W. G. Spitzer and C. A. Mead, J. Phys. Chem. Solids 25, 443 (1964).

9. D. Long and J. L. Schmidt, Semimetals and Semiconductors, ed. R. K. Willardson and A. C. Beer (Academic Press, New York, 1970), Vol. 5, Chap. 5.

10. D. J. Chadi, J. P. Walter, M. L. Cohen, Y. Petroff and M. Balkanski, Phys. Rev. B5, 3058 (1972).

11. M. L. Cohen and V. Heine, Solid State Physics 24, 37 (1970).

12. J. P. Walter and M. L. Cohen, Phys. Rev. B4, 1877 (1971).

13. G. Weisz, Phys. Rev. 149, 504 (1966).

14. S. Bloom and T. K. Bergstresser, Solid State Commun. 6, 465 (1968).

15. J. P. Walter, M. L. Cohen, Y. Petroff, and M. Balkanski, Phys. Rev. B1, 2661 (1970).

16. P. Löwdin, J. Chem. Phys. 19, 1396 (1951).

17. J. C. Woolley and B. Ray, J. Phys. Chem. Solids 13, 151 (1960).

18. J. L. Schmit and E. L. Stelzer, J: Appl. Phys. 40, 4865 (1969).

19. S. H. Groves, T. C. Harman, and C. R. Pidgeon, Solid State Commun. 9, 451 (1971).

20. C. Vérie, Proceedings of the 1967 Int. Conf. on II-VI Semiconducting Compounds, D. G. Thomas, ed. (Benjamin, N. Y., 1967), p. 1124.

21. E. O. Kane, J. Phys. Chem. Solids 1, 249 (1957).

22. A. Baldereschi, Bull. A. P. S., March 1972, p. 237.

23. W. Kohn, Phys. Rev. 115, 809 (1959).

24. E. I. Blount, in Advances in Solid State Physics, eds. F. Seitz and D. Turnbull (Academic Press, Inc., New York, 1962), Vol. 13, p. 305.

Figure Captions

Fig. 1. Variation of the energy gap E_G and spin-orbit splittings at Γ and L with alloying for $Hg_{1-x}Cd_xTe$ alloys.

Fig. 2. Band structures near Γ for HgTe, CdTe and two alloys near the semimetal-semiconductor transition region. The band structures extend from Γ to $|\vec{k}| = 0.18\,(\frac{2\pi}{a})$ in the Λ and Δ directions.

Fig. 3. HgTe charge densities near Γ for the Γ_8 conduction and valence levels (top), and the Γ_6 valence level (bottom).

Fig. 4. CdTe charge densities near Γ for the Γ_6 conduction level (top) and the Γ_8 valence level (bottom).

Fig. 5. Sum of valence band charge densities near Γ for HgTe, $Hg_{0.167}Cd_{0.833}Te$ and CdTe.

Fig. 6. Total valence band charge densities for HgTe and CdTe. These charge densities have been normalized to $8e/\Omega$.

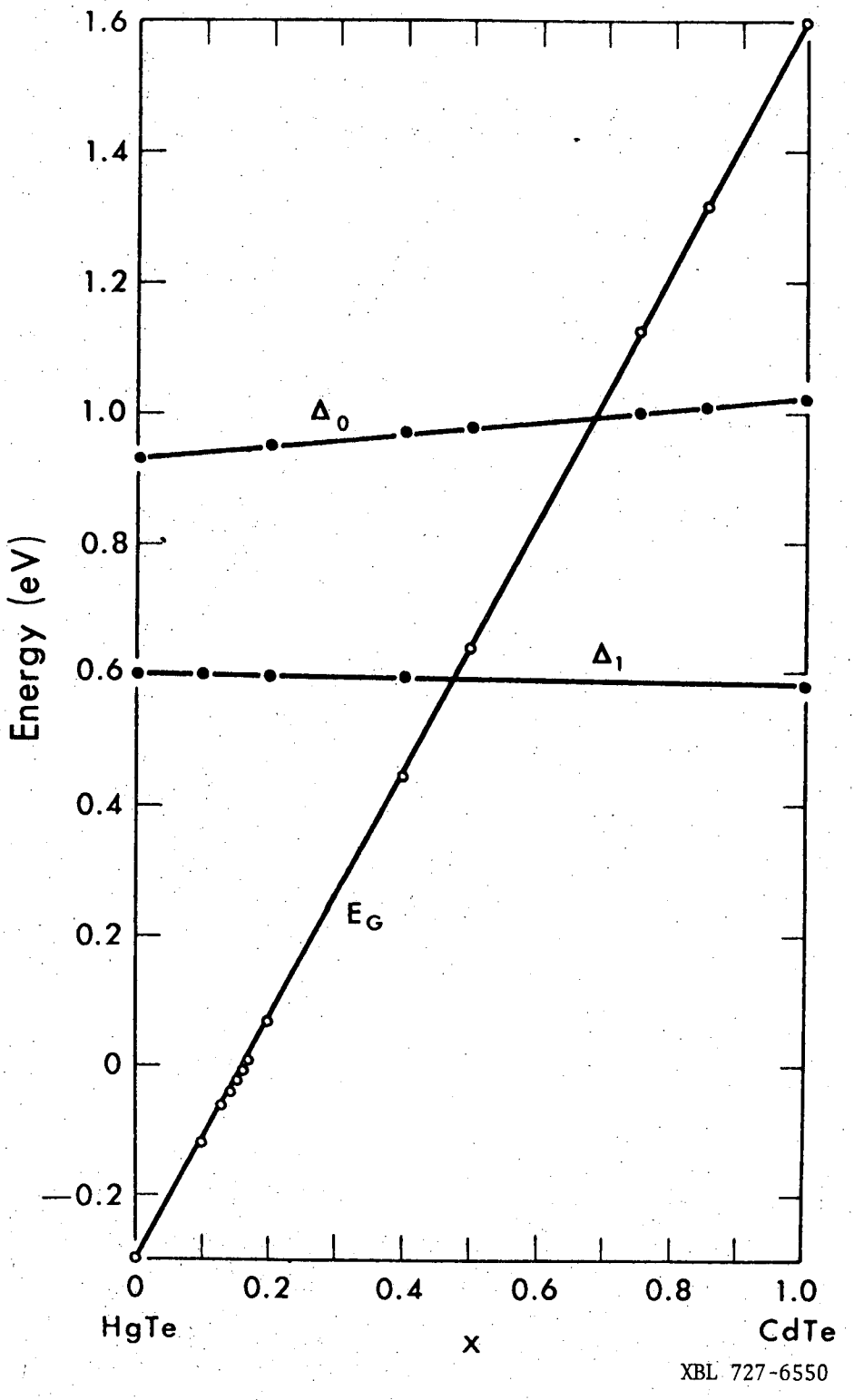
1.6
1.4
1.2
1.0
0.8
0.6
0.4
0.2
0
−0.2
Energy (eV)
Δ_0
Δ_1
E_G
0
0.2
0.4
0.6
0.8
1.0
HgTe
CdTe
x
XBL 727-6550

Fig. 1.

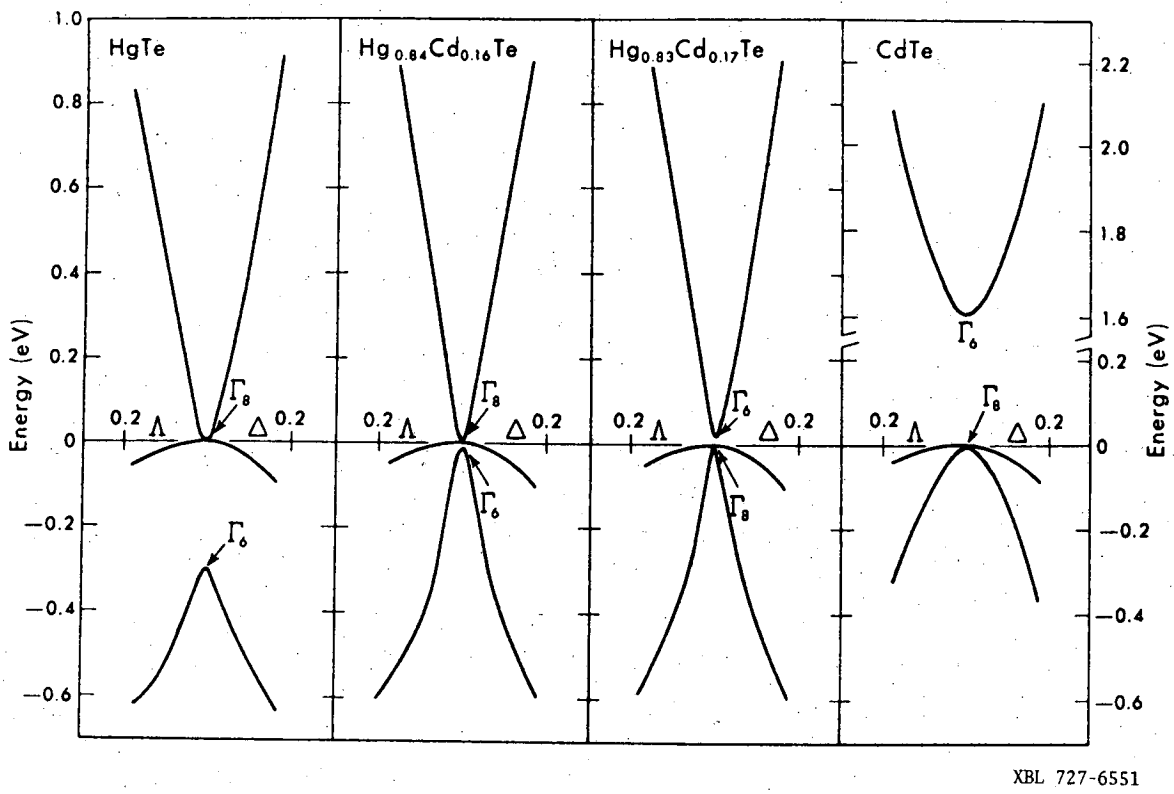
HgTe
$Hg_{0.84}Cd_{0.16}Te$
$Hg_{0.83}Cd_{0.17}Te$
CdTe
Energy (eV)
Energy (eV)
1.0
0.8
0.6
0.4
0.2
0
−0.2
−0.4
−0.6
2.2
2.0
1.8
1.6
0.2 Λ
Δ 0.2
Γ_8
Γ_6
XBL 727-6551

Fig. 2.

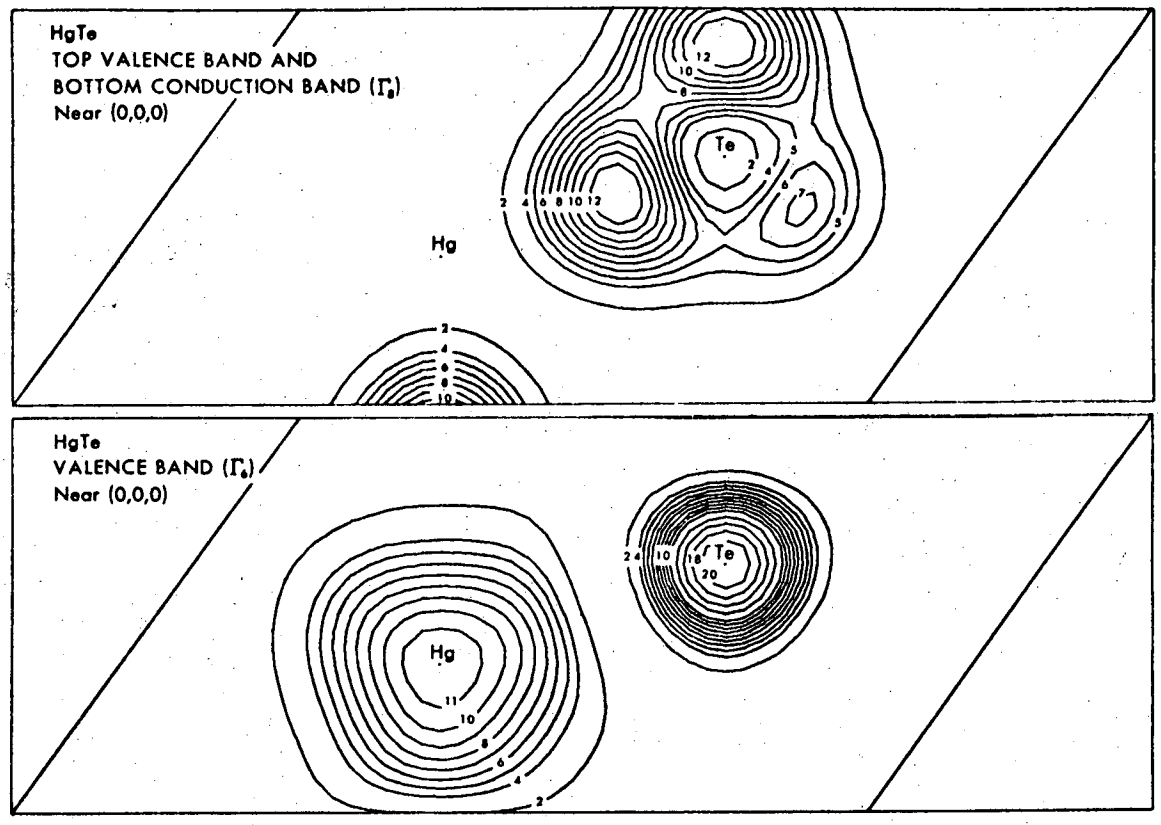

XBL 727-6552

Fig. 3.

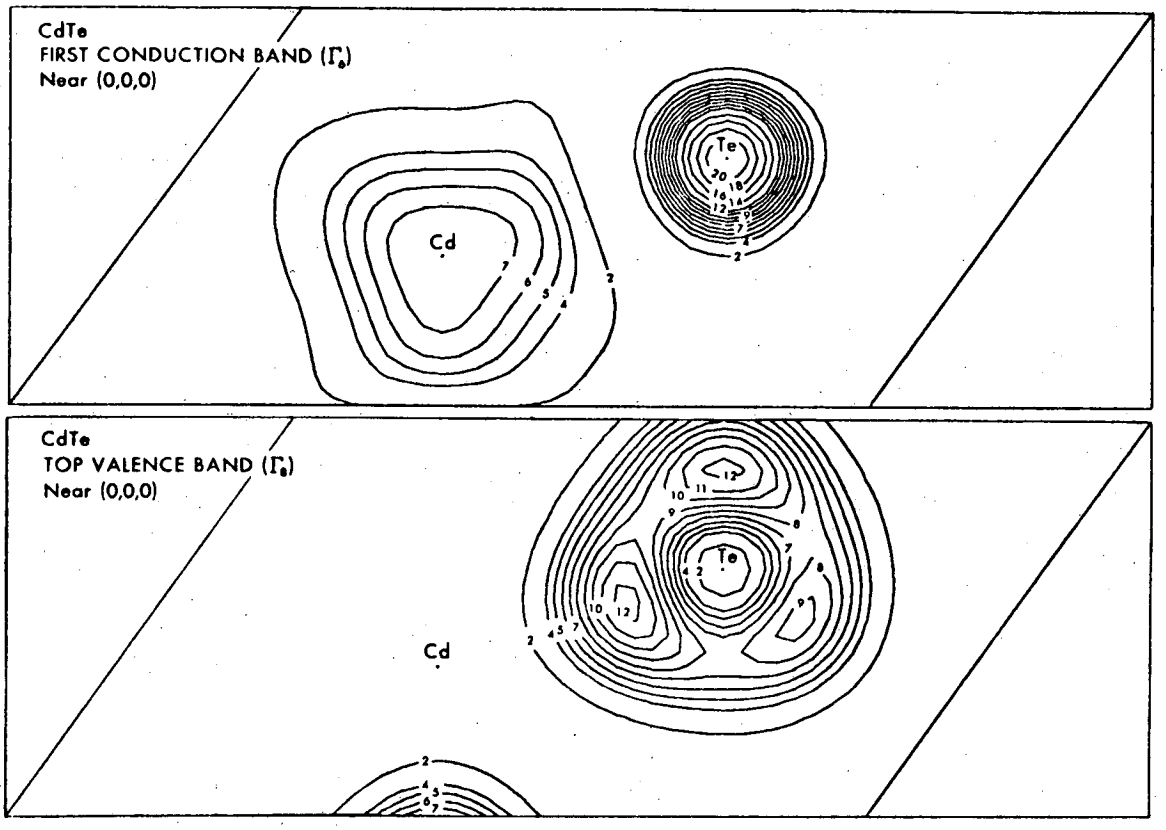

XBL 727-6553

Fig. 4.

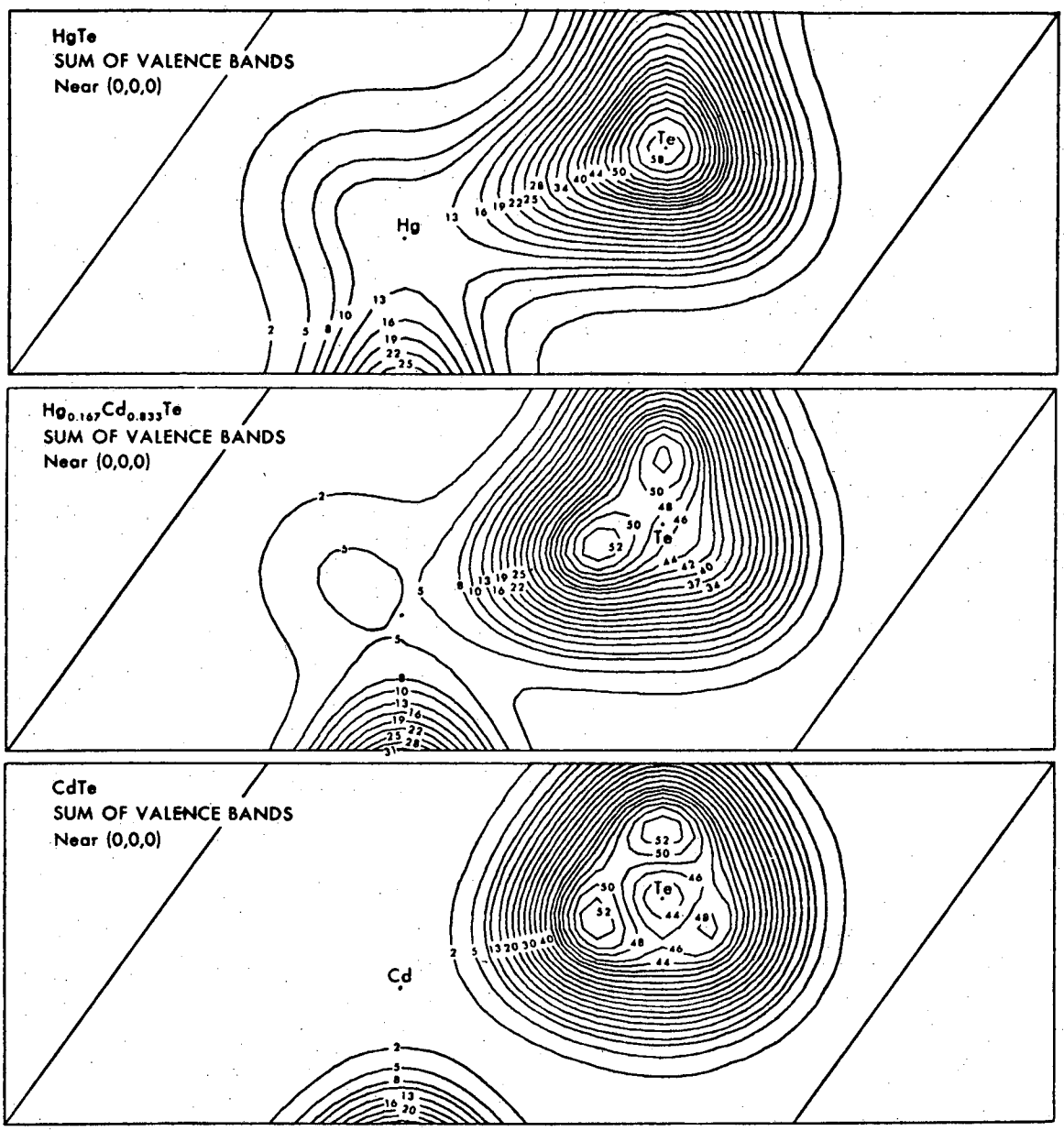

XBL 727-6554

Fig. 5.

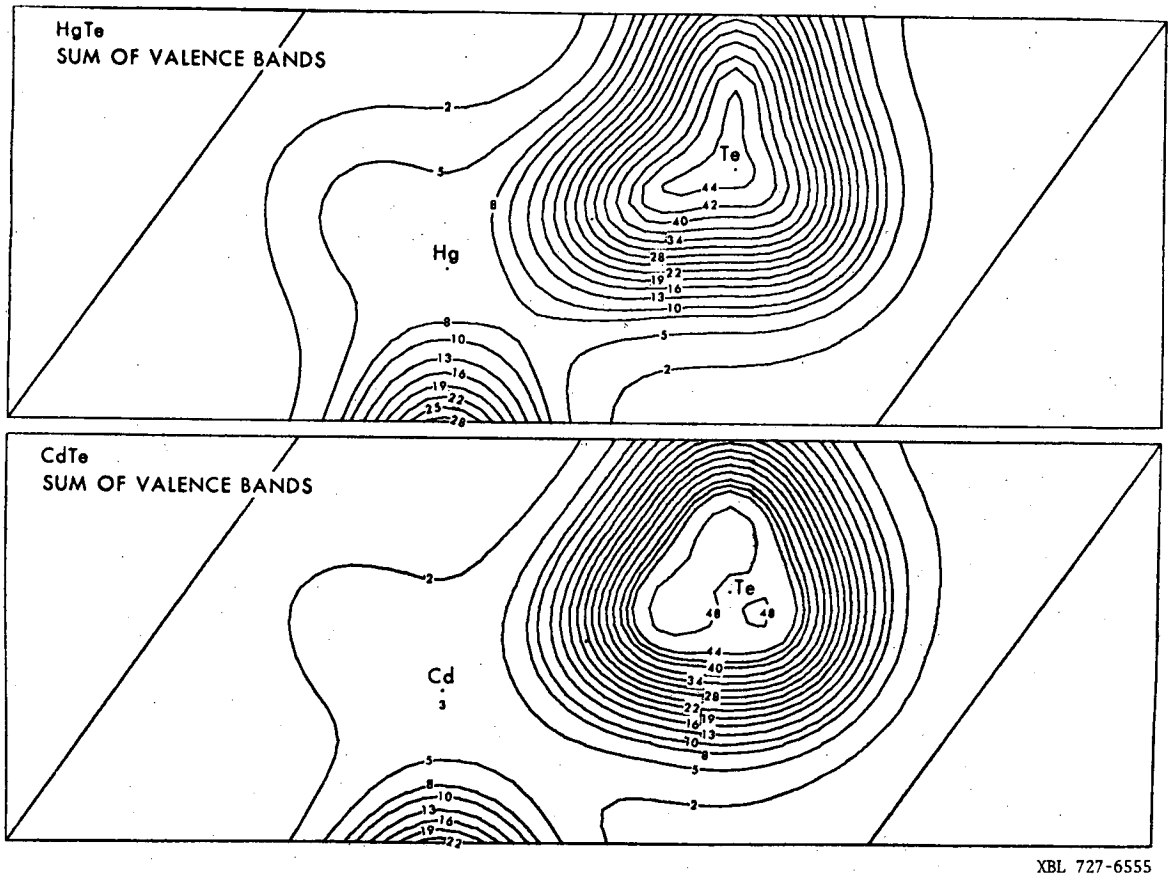
HgTe
SUM OF VALENCE BANDS
Te
Hg
CdTe
SUM OF VALENCE BANDS
Te
Cd
XBL 727-6555

Fig. 6.

TECHNICAL INFORMATION DIVISION
LAWRENCE BERKELEY LABORATORY
UNIVERSITY OF CALIFORNIA
BERKELEY, CALIFORNIA 94720